WEP Warwick Evans Publishing

Transactions on Computer Science and Intelligent Systems Research
ISSN: 2960-1800, eISSN: 2960-2238 | Volume 14
TPCEE 2026

Composition-Dependent Mass-Radius Relations of White Dwarfs and Their Astrophysical Applications

Derunzhou Xu *

Winchester College, Winchester, United Kingdom

* Corresponding Author Email: richardx4488@gmail.com

Abstract. The remnant of low to intermediate mass stars, white dwarfs, are supported by the electron degeneracy pressure, preventing the gravitational collapse. Their internal structure and observable properties depend sensitively on core composition through the mean molecular weight per electron, μ_e. The author used MATLAB to compute a flexible numeric solver that computes different core compositions of white dwarfs with different elemental mass fractions. μ_e was first calculated using exact atomic weights and their abundances in the white dwarf. Then integrates the equations of stellar structure using the full relativistic Chandrasekhar degeneracy pressure and produces a mass-radius curve for different compositions, including pure carbon, pure oxygen, carbon-oxygen mixtures, neon-rich, and iron cores. Results show that composition-driven changes in $\mu_e$produce measurable differences in maximum mass and radius at fixed mass. These structural variations directly affect cooling timescales, crystallisation onset, and pulsation periods of a white dwarf. The model is applied to white dwarf cosmochronology and to laboratory warm dense matter experiments where degeneracy-pressure predictions benchmark equation-of-state measurements under white-dwarf-like conditions.

Keywords: Electron degeneracy pressure; Fermi momentum; Mean molecular weight per electron; White dwarf.

1. Introduction

White dwarfs represent the final evolutionary stage for the vast majority of stars. Their structures are primarily supported by electron degeneracy pressure to prevent the strong gravitational collapse. The electron degeneracy pressure is strongly determined by their mean molecular weight per electron (μ_e), which in turn is determined by the core chemical composition. Accurate modelling of white dwarf structure for a range of different core mixtures is therefore essential for understanding stellar endpoints, Type Ia supernovae, and the use of white dwarfs as cosmic clocks.

The research on white dwarfs significantly advances with Chandrasekar's finding of the equation for electron degeneracy pressure, where the mass-radius relationship of white dwarfs can first be plotted. This resulting relation predicts that more massive white dwarfs have smaller radii, converging on the Chandrasekhar limiting mass of $\sim 1.44\, M_{\odot}$, which is one of the most fundamental predictions of quantum statistical mechanics applied to astrophysical objects [1]. More research on white dwarfs has been conducted since then. Recent research has progressed significantly in both theoretical and observational aspects of white dwarf structure and evolution while highlighting persistent challenges. Saumon et al. provide a comprehensive review of current problems in white dwarf physics, emphasising uncertainties in the equation of state for degenerate electrons and dense plasmas, the treatment of multi-element compositions (typically carbon–oxygen or oxygen–neon cores) [2]. These microphysical issues directly affect predicted mass–radius relations and cooling tracks. Raddi et al. provide a strong observational test using 50 hydrogen-atmosphere white dwarfs in common proper-motion binaries. By combining high-resolution spectroscopy ($R \approx 18{,}500$) for gravitational redshift measurements with photometric radii from Gaia, they show that the measured masses and radii agree within 6% at the 1σ level with the theoretical mass–radius relation, with less scatter than earlier work [3] such as Arseneau et al. (2024) [4]. In other applications, Pathak et al. quantify systematic

Content from this work may be used under the terms of CC BY-NC 4.0 licence (https://creativecommons.org/licenses/by-nc/4.0/).
Published by Warwick Evans Publishing.

uncertainties in white dwarf cooling ages arising from core chemical structure, envelope masses, and opacities [5].

This work develops a numerical solver for the white dwarf structure equations that computes mass-radius curves for different elemental core compositions of white dwarfs using Matlab simulation and the exact Chandrasekhar relativistic equation of state. The primary aim is to quantify and reproduce the results of how μ_e and core composition shift the MRR and the effective Chandrasekhar mass across astrophysically relevant element combinations. The applications of these results are then discussed, with the major application being in White Dwarf Cosmochronology and Core Crystallisation. A second application, relating the theoretical Fermi pressure baseline relevant to WDM experiments at laser facilities such as NIF, where C/O mixtures at white-dwarf densities are actively being studied, is also being discussed in the application.

2. Methodology

2.1. Setting up the conditions

2.1.1. Gravity

The major force acting on the white dwarf is its gravity and electron degeneracy pressure. The electron degeneracy pressure is the supporting force. The white dwarf is being pulled together by gravity, which 2 differential equations relating pressure and radius(r),and mass and radius$(r)$of the stellar object, can be constructed to express gravitational pressure. $\frac{dP}{dr} = -\frac{Gm(r)\rho(r)}{r^2}$. $\frac{dm}{dr} = 4\pi r^2\rho(r)$, where ρ is the density of the stellar object.

To avoid integrating pressure directly for simplicity, the equation of state (EOS)$(P(\rho))$ is used to rewrite the first equation as:

$$\frac{d\rho}{dr} = -\frac{Gm(r)\rho(r)}{r^2}\left(\frac{dP}{d\rho}\right)^{-1} \tag{1}$$

This gives a system where only variables m(r) and ρ(r) are considered. This means that only two first-order ODEs in MATLAB are needed.

2.1.2. Relativistic Degenerate gas

The pressure of a zero-temperature degenerate electron gas is given by

$$P(\rho) = C \cdot F(x), C = \frac{\pi m_e^4 c^5}{3h^3}, \tag{2}$$

where the function $F(x)$ is

$$F(x) = x(2x^2 - 3)\sqrt{1 + x^2} + 3\sinh^{-1}(x)\,. \tag{3}$$

Here, $x = p_F/(m_e c)$, with p_F being the Fermi momentum given by $p_F = \hbar(3\pi^2 n_e)^{1/3}$ in which n_e is the electron number density and μ_e is the mean molecular weight per electron given by $n_e = \frac{\rho}{\mu_e m_p}$. This expression of electron degeneracy pressure smoothly interpolates between the non-relativistic $\left(\left(P \propto \rho^{5/3}\right)\right)$ and ultra-relativistic $\left(\left(P \propto \rho^{4/3}\right)\right)$limits [1].

2.1.3. Fermi Momentum

Fermi momentum is the momentum of the highest occupied electron state at absolute zero. Electrons fill from the lowest momentum state $p = 0$ up to $p = p_f$, forming a sphere in momentum space. In three dimensions, the occupied states form a filled sphere in k-space (wavevector space) of radius $k_F = p_F/\hbar$. The formula $p_F = \hbar(3\pi^2 n_e)^{1/3}$ Is obtained by counting how many quantum states fit inside that sphere, given the density of states in k-space.

In three-dimensional k-space, each quantum state occupies a volume $(2\pi)^3/V$, where V is the volume of the system. The electrons fill all states up to the Fermi wavevector (k_F), defining a sphere in k-space of radius k_F. The total number of electrons N_e is given by the volume of this sphere multiplied by the density of states and spin degeneracy. $N_e = 2 \times \frac{V}{(2\pi)^3} \times \frac{4}{3}\pi k_F^3$, where the factor 2 accounts for the two possible spin states per momentum state.

Rearrange the formula with the electron number density ($n_e = N_e/V$), one obtains the equation $n_e = \frac{k_F^3}{3\pi^2}$. The Fermi momentum ($p_F$) relates to the Fermi wavevector by ($p_F = \hbar k_F$), therefore people can obtain the equation $p_F = \hbar(3\pi^2 n_e)^{1/3}$.

2.2. Numeric integration

The ODE integrated in MATLAB (ode45) is used for numeric integration of the differential equations. To find the stellar surface for the limit, define the boundary as the radius where the density falls below $10^{-6}\rho_c$ (where ρ_c is the density of the centre). This value is chosen due to the numerical stiffness of the hydrostatic equilibrium equation near the stellar surface. When $\rho \to 0$, standard ODE solvers encounter singularities as the derivative $dP/d\rho$ vanishes. To avoid non-convergence errors for the program, a relative surface density was determined such that the integration terminates when the local density drops to $\rho_{\text{bound}} = 10^{-6}\rho_c$. Numerical verification with the code proves that the setting of bounded density as $10^{-6}\rho_c$ introduces an error of less than 10^{-5} in both total mass and radius, which is negligible. Initial conditions are set at a small radius (r_0) to avoid singularities as well:

$$r_0 = 10^{-6}\text{meters}, m(r_0) = \frac{4}{3}\pi r_0^3 \rho_c, \rho(r_0) = \rho_c \quad (4)$$

Central densities are swept logarithmically from (10^7) to $(10^{13})\ \text{kg m}^{-3}$. For each (ρ_c), The integration yields a total mass (M) and radius (R). Then the mass-radius curve is plotted for each of the different element composition cores.

The maximum density of the core is set to 10^{13}, where a typical white dwarf has densities of around 10^9 [2], the density of 10^{13} is an approximation set as the maximum density, and this density will lead to the collapse of the white dwarf's core.

2.3. Core composition

Cores of different elemental composition is constructed and plotted on the mass radius relationship core. Including pure carbon core, pure oxygen-16 core, pure helium-4 core, Neon-rich core (50 percent of oxygen-16 and 50 percent Neon-22), and a range of percentage mixtures of carbon and oxygen. A heavy core of pure Iron is also plotted to compare the Chandrasekhar limit of a heavier element. Using the ODE function of MATLAB, the graph of mass against radius and the Chandrasekhar limit can be found numerically. The data used for the molecular masses of these elements listed in Table 1 are from the National Institute of Science and Technology to 6 decimal places [6].

Table 1. relative atomic masses of different isotopes [6].

Element Isotope	Relative atomic mass
Helium – 4	4.002603
Carbon – 12	12.000000
Oxygen – 16	15.994915
Neon – 20	19.992440
Iron – 56	55.934937

3. Discussion of results

3.1. Overview of the mass-radius behaviour

The mass radius curve plotted for different compositions exhibits the characteristic of inverse relationship between the mass and the radius of the white dwarfs, see Fig. 1. This is a result of increasing mass causing the increase in density, pushing electrons into higher momentum states and increasing degeneracy pressure. The gradient of the curve decreases with greater density as the behaviour of the electrons becomes more relativistic, transitioning from $\left(P \propto \rho^{5/3}\right)$ to $\left(P \propto \rho^{4/3}\right)$ more.

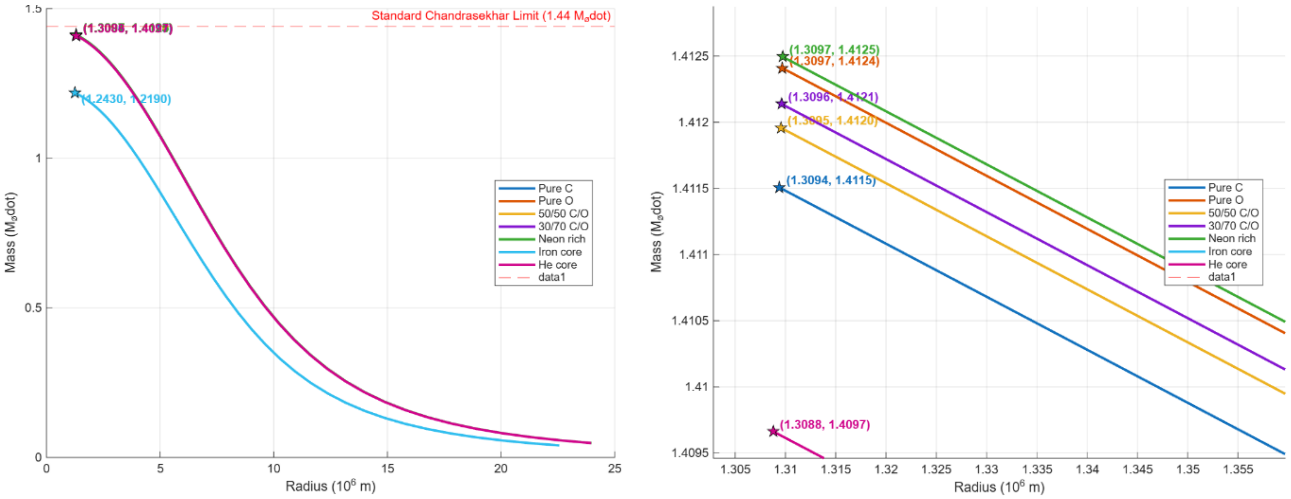

Fig. 1 Left: The mass against radius graph of white dwarf with different core compositions. Right: Zoom in of the mass radius graph where the top curve is not clearly separated.

3.2. Effect of composition on mass-radius curves

The mass radius graph of a white dwarf is plotted. Due to the similar mass-to-charge ratios of Carbon, oxygen, helium, and neon, the mass-radius curve for these elements does not show a clear separation. With curves closely together.

The mass of the white dwarfs does not reach the standard Chandrasekhar limit in the program. This is a result of the boundary condition set for the core and the edge of the white dwarf. Since a maximum density is set for the centre, the mass radius curve will not intercept the y-axis of the mass. Reaching a radius of 0 for the white dwarf implies infinite density, which only exists theoretically. Another boundary condition for the edge of the white dwarf is set as $10^{-6}$of the centre density to avoid the singularity of the $\frac{dP}{d\rho}$. This means that a small mass at the surface of the white dwarf or the atmosphere of the white dwarf is excluded. So, the sum of the mass will be slightly smaller than the Chandrasekhar limit. The results in Table 2 are the analytical results of the Chandrasekhar limit for the same compositions

For each composition, the mass asymptotically approaches a maximum value as ρ_c increases. The numerical limiting masses agree with the analytic scaling to within 3 percent. This percentage difference arises from the comparison between the numerical integration results and the analytic Chandrasekhar limit formula. This confirms the validity of the EOS and integration method.

Table 2. Analytic results of the Chandrasekhar limit of different core compositions.

Core composition	Mean molecular weight per electron (μ_e)	Chandrasekhar Limit/$M_\odot$
Pure C-12	2.0000	1.440
Pure O-16	1.9994	1.441
50/50 C-12/O-16	1.9997	1.440
30/70 C-12/O-16	1.9996	1.441
Neon rich (50/50 O-16/Ne-22)	1.9993	1.441
Iron core (Fe-56)	2.1513	1.245
He core (He-4)	2.0013	1.438

3.3. Approaching the Chandrasekhar limit

The data used of the atomic masses are corrected to 6 decimal places, assuming specific isotopes of the elements; for example, only carbon-12 is considered in the pure carbon composition of the white dwarf core. The accurate data used allows the lines to separate for carbon, oxygen, helium and neon since the $\mu_e$of these elements are all 2 if only approximations are used. Using this exact data resulted in slightly different μ_e. This resulted neon having the highest mass with its smallest μ_e. While helium has the highest μ_e make it the lowest mass in the cluster of the elements.

3.4. Comparison with modern observations

The composition of white dwarfs observed mostly clusters around the C/O sequence [2]. Supporting the assumptions of the different composition of carbon and oxygen core.

For He-rich core white dwarfs, typically formed in binary evolution, it matches the larger-radius (same mass, larger radius) predictions of the model [7,8]. The model's predictions are consistent with theoretical expectations for such objects.

Fe-core white dwarfs are rare but may arise in extreme accretion scenarios. observational evidence that iron-rich material reaches white dwarfs through external accretion rather than internal stellar evolution [9]; Therefore, the iron-core white dwarf modelled in this work therefore represents an extreme theoretical end-member that probes the maximum possible μ_e and minimum radius for a given mass, rather than a common astrophysical population.

4. Applications

4.1. White Dwarf Cosmochronology and Core Crystallisation

The major application of this composition-dependent model of white dwarfs is in galactic cosmochronology. A white dwarf does not undergo internal nuclear fusion. Throughout a white dwarf's stellar life, it is purely undergoing monotonic cooling. By measuring a white dwarf's current luminosity and effective temperature, and comparing it against theoretical structural models, the "cooling age" can be determined for this white dwarf [10], which makes them a powerful cosmic clock for dating the Galactic disk, open clusters, globular clusters, and star-formation histories.

As a white dwarf cools, its ions undergo a first-order liquid-to-solid phase transition, releasing latent heat and gravitational energy that slows the cooling rate. Tremblay et al. (2019) confirmed this observationally via a pile-up in the Gaia cooling sequence [11]. The onset density of crystallisation is set by μ_e, meaning the C/O and Ne-rich curves computed here crystallise at different times and release different amounts of energy. In C/O cores, Ne impurities form buoyant crystals that float upward and release additional gravitational energy, interrupting cooling for several Gyr [12]. This mechanism is absent in O/Ne cores, where crystallisation proceeds normally with no significant extra delay [13].

To determine the cooling age of the white dwarf. The internal composition is needed. With the accurate mass-radius diagram of the different compositions of the white dwarfs, the element composition of the white dwarfs can be determined, given the known mass and size. The mass-radius relation computed in this work is a crucial tool for this method, since observed radii must be converted to masses before evolutionary cooling tracks can be applied.

The mean molecular weight per electron μ_e, computed in the program from mass fractions and exact atomic weights for mixtures, directly affects the electron degeneracy pressure and the resulting mass-radius relation. Each of the exact atomic weights for mixtures, including pure C, O, C/O blends, Ne-rich, and Fe cores, all directly affects the electron degeneracy pressure through the Chandrasekhar $F(x)$ function, this sets an accurate mass-radius curve for all compositions that is helpful for this area.

4.2. Warm dense matter

The research into warm dense matter (WDM) is another key application of the model. Warm dense matter occurs in the interiors of giant planets, white dwarf atmospheres and in the early stages of inertial confinement fusion (ICF) experiments. Understanding the relationship between pressure, density and temperature in WDM is central to both laboratory physics and astrophysics.

The electron degeneracy computed with MATLAB, using the Chandrasekhar function, represents the zero-temperature theoretical baseline of which WDM behaviour is measured. In ICF experiments, the fuel adiabat parameter $\alpha$is formally defined as the ratio of the actual shell pressure to the Fermi-degenerate pressure at solid density [14].

The relevant connection of this model with WDM comes from Kritcher et al. (2020), who used the National Ignition Facility (NIF) to measure the equation of state of carbon in white dwarf conditions. They reported measurements of the relationship between pressure and density along the principal shock Hugoniot of hydrocarbon to within five per cent, relevant for pressures ranging from 100 million to 450 million atmospheres [15]. Their data agreed with EOS models which include detailed electronic shell structure, demonstrating the enhanced compressibility due to pressure ionization of carbon's inner-shell electrons relative to models without this effect. The MATLAB program in this work computes the pure Chandrasekhar degenerate electron pressure, $P(\rho)$, which assumes a zero-temperature, fully ionised, non-interacting electron gas. This is a simpler theoretical limit than the finite-temperature, partially-ionised EOS with electronic shell corrections that Kritcher et al. (2020) tested experimentally.

5. Conclusion

The numerical simulation was programmed with the support of MATLAB of a white dwarf with different core compositions. By integrating the equations of hydrostatic equilibrium and mass continuity with Chandrasekhar's exact relativistic degenerate-electron equation of state, code in MATLAB language is used to reproduce the inverse mass- radius relationship and compute the detailed μ_e using specific isotopic masses. For elements with a μ_e of approximately 2 (pure C, pure O, C/O, He, and Ne-rich cores), the maximum mass approaches 1.44 $M_{\odot}$. For iron core, where $\mu_e \approx 2.15$, a limit of approximately a maximum of 1.24 $M_{\odot}$. The model assumes the stellar temperature to be zero Kelvin for fermi gas, which is relatively accurate near the core of the white dwarf. However,

when the density of the white dwarf decreases as the program integrates away from the centre, the temperature is no longer around absolute zero. The assumption of perfect spherical symmetry, non-rotating stars, and uniform composition is also made. Even though the effect is minor, it can still introduce a small error in more extreme bodies.

Further research to make the model more accurate by including finite-temperature effects, rotation, and strong magnetic fields can be conducted to eliminate errors in the result. At finite temperatures, thermal pressure inflates white dwarf radii beyond the zero-temperature prediction, particularly in low-mass objects. For spinning white dwarfs, it is reported that rotation provides additional centrifugal support against gravity, raising the effective mass limit and affecting radii across the full mass range. These extended conditions can be considered and integrated into the model and directly tested against observations, for example with the GAIA satellite database TESS satellite which is used to determine the internal composition of white dwarfs through pulsation frequencies. ESA's PLATO mission, launching in 2026, will further help to sharpen these observations.

References

[1] Chandrasekhar S. The highly collapsed configurations of a stellar mass (second paper). Mon Not R Astron Soc. 1935;95(3):207-225.

[2] Saumon D, Blouin S, Tremblay PE. Current challenges in the physics of white dwarf stars. Phys Rep. 2022;988:1-63.

[3] Raddi R, Rebassa-Mansergas A, Torres S, et al. Testing the mass-radius relation of white dwarfs in common proper-motion pairs. Astron Astrophys. 2025;695:A131.

[4] Arseneau S, Chandra V, Hwang HC, et al. Measuring the mass–radius relation of white dwarfs using wide binaries. Astrophys J. 2024;963(1):17.

[5] Pathak P, Blouin S, Herwig F. Quantifying systematic uncertainties in white dwarf cooling age determinations. Astrophys J. 2025;983(2):158.

[6] National Institute of Standards and Technology. Atomic weights and isotopic compositions for all elements. NIST. Accessed July 14, 2026. https://physics.nist.gov/cgi-bin/Compositions/stand_alone.pl

[7] Zhang Y, Li Z, Chen X. Formation of extremely low-mass white dwarfs in wide orbits. arXiv. Preprint posted online 2025. arXiv:2511.15993.

[8] Scalco M, Salaris M, Bedin LR, et al. JWST imaging of omega Centauri: II. Evidence for a split white dwarf cooling sequence in the near-infrared. arXiv. Preprint posted online 2025. arXiv:2510.08715. doi:10.48550/arXiv.2510.08715

[9] Bonsor A, Lichtenberg T, Drążkowska J, Buchan AM. Rapid formation of exoplanetesimals revealed by white dwarfs. Nat Astron. 2022;7(1):39-48.

[10] Fontaine G, Brassard P, Bergeron P. The potential of white dwarf cosmochronology. Publ Astron Soc Pac. 2001;113(782):409-435.

[11] Tremblay PE, Fontaine G, Fusillo NPG, et al. Core crystallization and pile-up in the cooling sequence of evolving white dwarfs. Nature. 2019;565(7738):202-205.

[12] Bédard A, Blouin S, Cheng S. Buoyant crystals halt the cooling of white dwarf stars. Nature. 2024;627(8003): 286–288.

[13] Barrientos M, Kilic M, Bergeron P, Blouin S, Brown WR, Andrews JJ. Fundamental tests of white dwarf cooling physics with wide binaries. Astrophys J. 2024;973(2):88.

[14] Trickey W, Goncharov VN, Betti R, et al. The physics of gain relevant to inertial fusion energy target designs. Phys Plasmas. 2024;31(1):012702.

[15] Kritcher AL, Swift DC, Döppner T, et al. A measurement of the equation of state of carbon envelopes of white dwarfs. Nature. 2020;584(7819):51-54.